ELECTROCHEMICAL INVESTIGATION OF OCTAETHYL PORPHYRIN IRON(III) CHLORIDE IN THE PRESENCE OF PYRIDINE, IMIDAZOLE AND COLLIDINE: AN APPROACH TO THE ROLE OF PYRIDINE IN THE COUPLED OXIDATION

N. Safari*, E. Nikpoor and M. Khorasani

Department of Chemistry, Shahid Beheshti University, Tehran, Islamic Republic of Iran

Abstract

Cyclic voltammogram and differential pulse polarograph of octaethyl porphyrin iron(III) chloride in dichloromethane was investigated in the presence of pyridine, imidazole and collidine. Values of $E_{1/2}$ for Fe^{III}/Fe^{II} redox reaction were monitored as a function of axial group concentration, and on the basis of these data, an overall oxidation-reduction and ligand addition scheme was formulated. Addition of pyridine resulted in anodic shift for oxidation wave from –0.16 V to –0.06 V while for imidazole and collidine we observed a cathodic shift.

Introduction

For degradation of heme into biliverdin there are two general pathways: *i*) A biological pathway [1,2] that utilizes heme oxygenase and dioxygen to convert heme to biliverdin, and biliverdin reductase which reduces biliverdin to bilirubin in the presence of NADPH-cytochrom-c Scheme 1. *ii*) A chemical system, oxidation of heme in pyridine by dioxygen in the presence of a reducing agent, hydrazine or ascorbic acid, which has been extensively used as a model for the heme oxygenase reaction [3-10]. This process, which is termed coupled oxidation, is proved to occur through a sequence of intermediate shown in Scheme 2. Pyridine as both solvent and source of axial ligands, has a major role in converting heme to biliverdin in this process. Protoheme undergoes negligible coupled oxidation in the absence of pyridine. Balch and co-worker [11] have recently shown that addition of $OEPFe^{III}Cl$ to methanolic solution of ascorbic acid and potassium cyanide leads to the production of verdoheme.

Electrochemical techniques for measuring porphyrin redox potentials have been used for some time [12,13]. The nature of the Fe^{III} counter ion, solvent system, axial ligation and the porphyrin ring basicity will influence

Keywords: Electrochemistry; $OEPFe^{III}Cl$; Coupled oxidation and pyridine

Abbreviations: TBAP: Tetrabutylammonium perchlorate; TBACI: Tetrabutylammonium chloride; $OEPFe^{III}Cl$: Octaethyl porphyrin iron(III) chloride; CV: Cyclic voltammetry; py: pyridine; Im: Imidazole; tmpy: 2,4,6-Trimethyl pyridine

* *E-mail: n-safari@cc.sbu.ac.ir*

Scheme 1

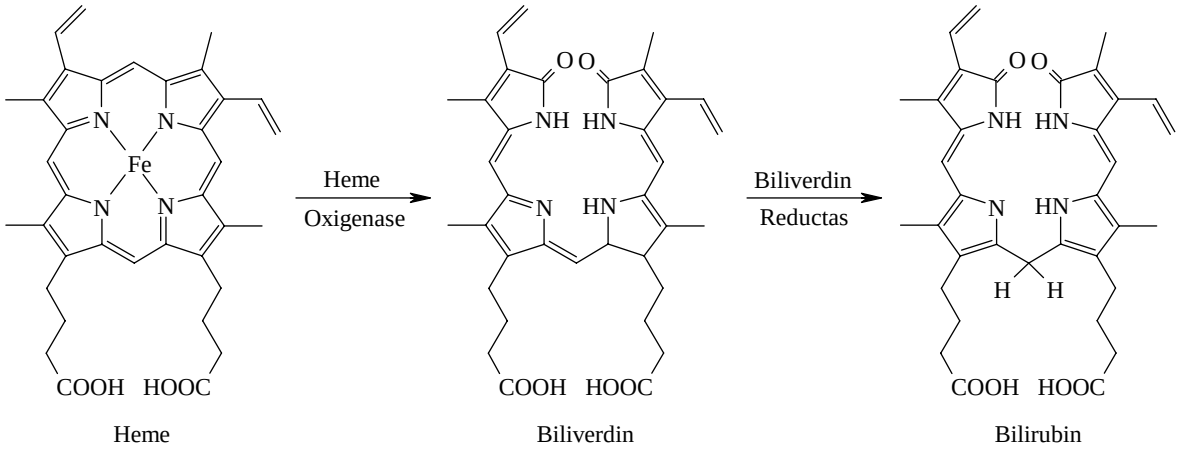

Scheme 2

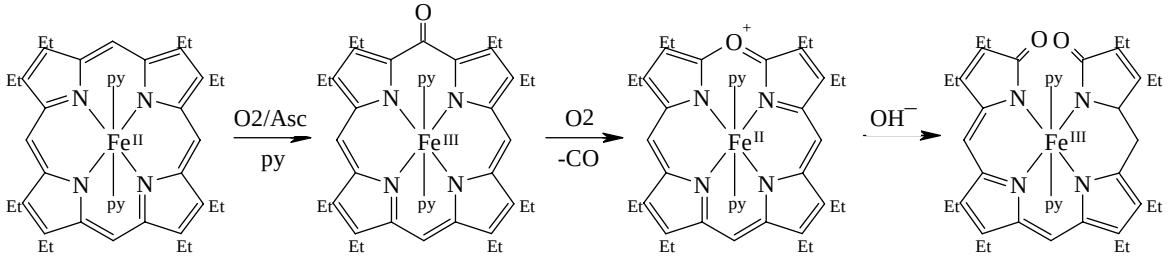

the spin state of the iron(III) atom, and this will be reflected in the spectroscopic or electrochemical properties of a given complex [14]. Both the nature of the Fe(III) counter ion and the solvent system have a strong effect on standard potential for the reaction Fe^{III}/Fe^{II}. A smaller effect is seen for the reaction Fe^{II}/Fe^{I}, and almost no effect for reactions involving oxidation of Fe(III) [15].

Two approaches have been used in investigating the relationship between redox potentials and axial ligation [15]. The first, and the most simple, is to complex the porphyrin axially under known experimental solution conditions and to measure the redox potential under these conditions. Absolute values of $E_{1/2}$ may then be related to a given set of axial ligands. The second approach is to complex the porphyrin axially (either the oxidized or reduced form) under a set of varying experimental conditions and, as a function of shifts of $E_{1/2}$ with these varying conditions (for example an increase in ligand concentrations), determine the stoichiometry and formation constants for addition of the ligand to the porphyrin molecule. In the first case the interest is in determining a given $E_{1/2}$; in the second case half-wave potentials are used to determine the complex which exists under a specific set of experimental conditions and to evaluate the magnitude of the formation constants for the addition of one or two ligands to the porphyrin center [15].

This article is concerned with electrochemical studies of heme in the presence of pyridine, imidazole and collidine, to understand the role of pyridine in the heme degradation process. We have observed that pyridine results in Fe^{III}/Fe^{II} reduction wave shift toward the anode whereas imidazole and collidine cause in cathodic shift in Fe^{III}/Fe^{II} reduction wave. This may be a clue to the role of pyridine in the heme degradation process.

In all voltammograms, we used CH_2Cl_2 as the solvent because there is no solvent complexation of Fe^{III} or Fe^{II}, and the potential range of this solvent is sufficient to view the Fe^{III}/Fe^{II} redox reaction of monomeric iron complex.

Results and Discussion

Reduction of $OEPFe^{III}Cl$ in Dichloromethane in the Presence of Pyridine

Cyclic voltammograms of $OEPFe^{III}Cl$ were taken in CH_2Cl_2 solutions containing various concentration of

pyridine. Representative voltammograms in CH_2Cl_2, in pyridine/CH_2Cl_2 mixture are shown in Figure 1. Cyclic voltammogram obtained of $OEPFe^{III}Cl$ is shown in Figure 1a. The peak potentials observed for the $Fe^{III}\rightarrow Fe^{II}$ couple in CH_2Cl_2 is at –0.47 V and $Fe^{II}\rightarrow Fe^{III}$ are at –0.35 V and –0.11 V *vs.* Ag/AgCl electrode (Figure 1a). Two anodic waves are due to oxidation of $[OEPFe^{II}Cl]^-$ (a_1) and $OEPFe^{II}$ (a_1') as shown in Scheme 3 [15]. Cyclic voltammogram obtained for neat pyridine is shown in Figure 1g, and dose not have any wave at the range 0.50 V to –1.00 V.

Addition of pyridine to a solution of $OEPFe^{II}Cl$ in CH_2Cl_2 result in splitting the Fe^{III}/Fe^{II} couple (Figure 1b-1f). Increasing pyridine concentration from 1:10 mole ratio to 10:1 mole ratio of pyridine caused the split peaks to move in opposite directions. Oxidation wave of $a_2\Leftrightarrow c_2$ has shifted anodically from –0.16 V to –0.06 V *vs.* Ag/AgCl reference electrode. On the other hand, reduction wave of $a_1\Leftrightarrow c_1$ has shifted catodically from -0.47 V to -0.57 V. Scheme 4 summarizes these changes.

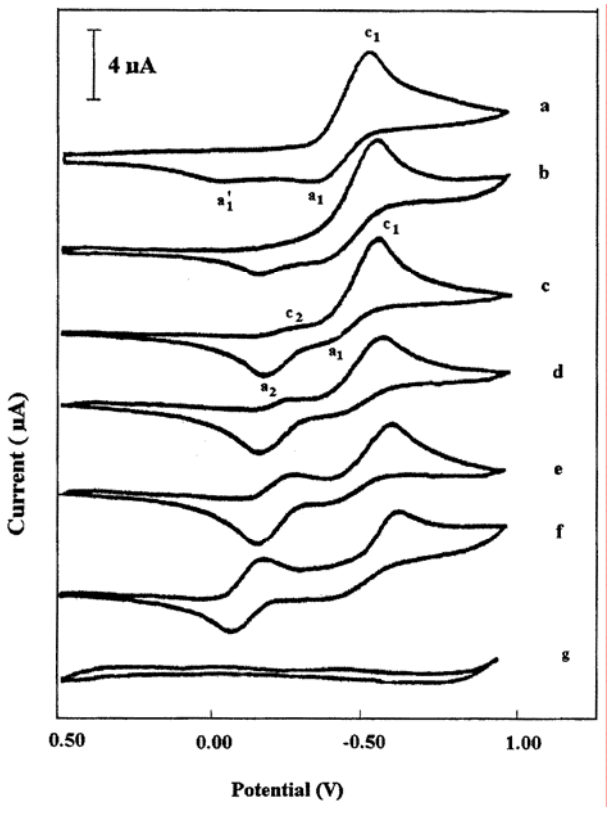

Figure 1. Cyclic voltammograms of $OEPFe^{III}Cl$, 1×10^{-3}M in dichloromethane in the presence of 0.1 M TBAP and different concentrations of py: (a) 0.00 M, (b) 1×10^{-4}M, (c) 2×10^{-4}M, (d) 1×10^{-3}M, (e) 5×10^{-3}M, (f) 1×10^{-2}M, and (g) Cyclic voltammogram of neat pyridine. The scan rate is 100 mV/s.

Addition of pyridine to $OEPFe^{III}Cl$ produces $[OEPFe^{III}Cl(py)]$ which reduced at c_1 to form $[OEPFe^{III}Cl(py)]^-$. This couple is more quasi-reversible in high concentrations of pyridine than in low concentrations. Second waves, $[OEPFe^{III}(py)_2]^+/[OEPFe^{II}(py)_2]$, are reversible and come at a lower cathodic potential due to increased stability of $[OEPFe^{II}(py)_2]$ in the pyridine solution. With increasing pyridine concentration, intensities of the latter wave increases in comparison to $[OEPFe^{III}Cl(py)]/[OEPFe^{II}Cl(py)]^-$, as expected. The differential pulse polarograms of these species, in the same condition as CV, are illustrated in Figure 2 and demonstrated the same behaviour.

Plot of $E_{1/2}$ (from differential pulse polarography) for $a_1\Leftrightarrow c_1$ couple *vs.* log[py] for the titration of $OEPFe^{III}Cl$ with pyridine in CH_2Cl_2 is shown in Figure 3. Slope of this plot is 49 mV and according to equation

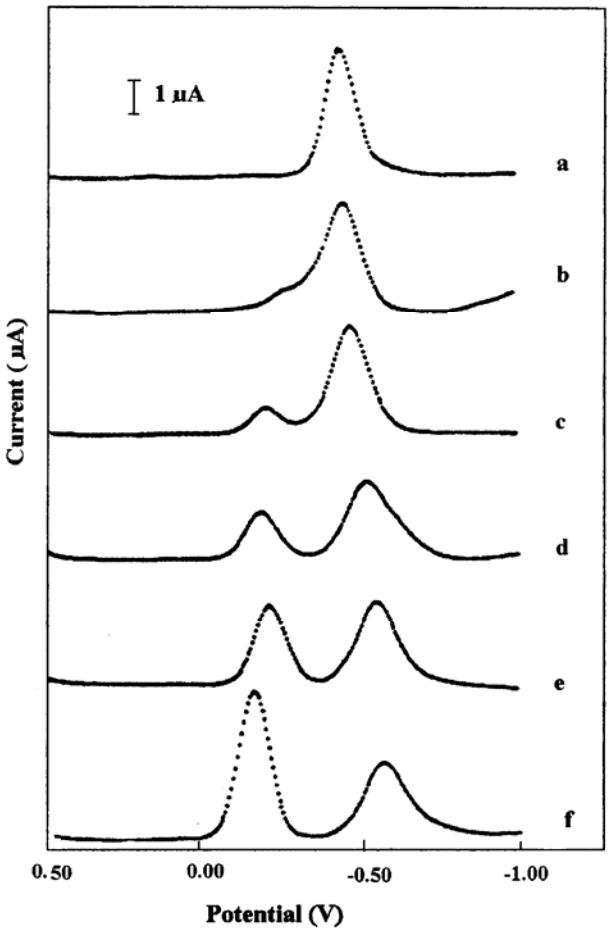

Figure 2. Differential pulse polarograms of $OEPFe^{III}Cl$, 1×10^{-3}M in dichloromethane in the presence of 0.1 M TBAP and different concentrations of py: (a) 0.00 M, (b) 1×10^{-4}M, (c) 2×10^{-4}M, (d) 1×10^{-3}M, (e) 5×10^{-3}M (f) 1×10^{-2}M.

Scheme 3

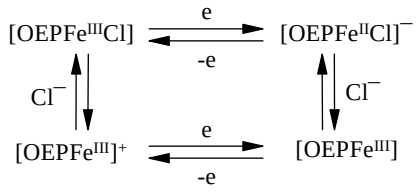

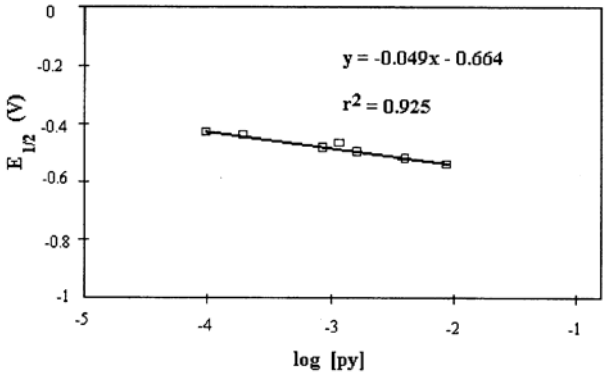

Figure 3. Plot of $E_{1/2}$, from differential pulse polarography, for $[OEPFe^{III}Cl(py)]/[OEPFe^{II}Cl(py)_2]$ couple *vs.* log[py].

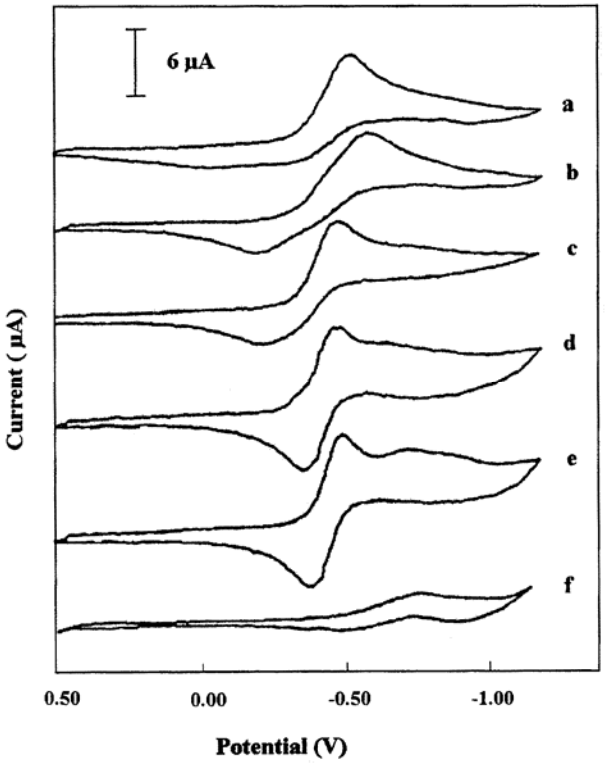

Figure 4. Cyclic voltammograms of $OEPFe^{III}Cl$, 1×10^{-3}M in dichloromethane in the presence of 0.1 M TBAP and different concentrations of Im: (a) 0.00 M, (b) 1×10^{-4}M, (c) 1×10^{-3}M, (d) 2×10^{-3}M, (e) 5×10^{-3}M, (f) Cyclic voltammogram of neat Im. The scan rate is 100 mV/s.

Scheme 4

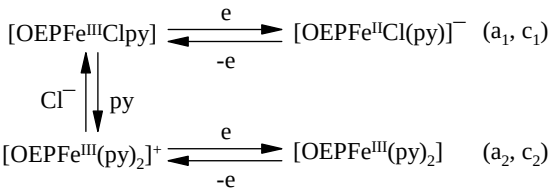

$\frac{\Delta E_{1/2}}{\Delta \log[L]} = \frac{0.059p}{n}$ is closed enough to 59 mV for when *n*, number of exchanged electrons and *p*, number of exchanged ligands are 1 [16].

Reduction of $OEPFe^{III}Cl$ in Dichloromethane in the Presence of Imidazole

Reduction of $OEPFe^{III}Cl$ in the presence of different amounts of imidazole, (Im) was investigated by cyclic voltammetry and differential pulse polarography. By addition of Im, oxidation waves at -0.11 V, and -0.35 V disappeared. Increasing concentrations of imidazole from 1:10 mole ratio (Fig. 4b) to 5:1 mole ratio (Fig. 4e) resulted in shifting of the oxidation wave from -0.16 V to -0.41 V and in high concentration of Im, redox reaction was reversible. Unlike pyridine, no splitting redox couple or anodic shift was observed (Fig. 4). The difference in electronic properties between pyridine and imidazole, gives rise to different behavior of these ligands toward Fe(III) porphyrins. Conflicting opinions as to π-donor/π-acceptor character of these two classes of bases have therefore been expressed by different investigators [17].

A new wave for reduction of free imidazole is observed around E_c=-0.75 V which obscure any possible metal porphyrin redox couple in that region. Observation of only one couple of oxidation-reduction in the presence of imidazole could be explained by production of only one species $[OPEFe^{III}(Im)_2]Cl$ in this solvent [18] (Scheme 5). On the other hand, in pyridine titration experiments, due to the lower coordination ability of pyridine, there is a competition between pyridine and chloride anion as axial ligands, and thereby two waves are observed.

Reduction of $OEPFe^{III}Cl$ in Dichloromethane in the Presence of Trimethyl Pyridine (Collidine)

Cyclic voltammetry of $OEPFe^{III}Cl$ in dichloromethane with collidine results in splitting of oxidation reduction couple to two pairs (Fig. 5). One is $a_1 \Leftrightarrow c_1$ at -0.45 V, which is fixed during the addition of collidine, that may result from the reaction of uncoordinated collidine ($OEPFe^{III}Cl$/ $OEPFe^{III}$). The other is $a_2 \Leftrightarrow c_2$ which is an oxidation-reduction couple for the coordinated form of collidine. Increasing the

concentration of collidine from 5:1 (Fig. 5b) to 15:1

Scheme 5

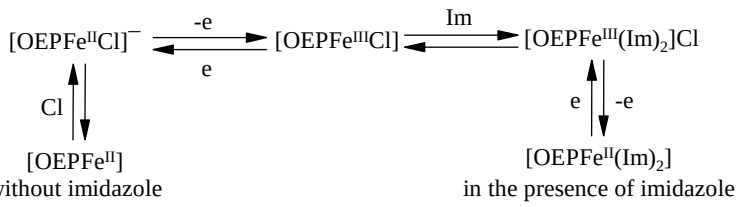

Scheme 6

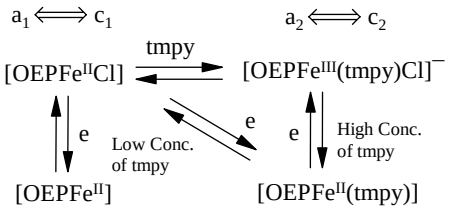

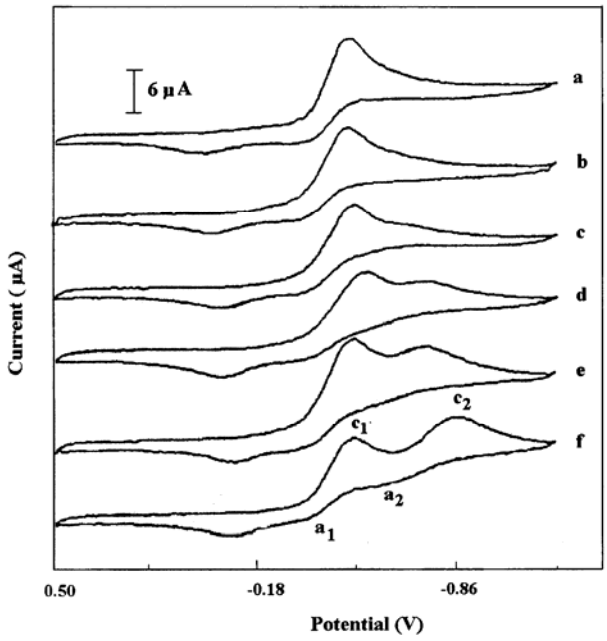

Figure 5. Cyclic voltammograms of $OEPFe^{III}Cl$, 1×10^{-3}M in dichloromethane in the presence of 0.1 M TBAP and different concentrations of tmpy: (a) 0.00 M, (b) 5×10^{-3}M, (c) 1×10^{-2}M, (d) 1.5×10^{-2}M, (e) 2.5×10^{-2}M, (f) 3×10^{-2}M. The scan rate is 100 mV/s.

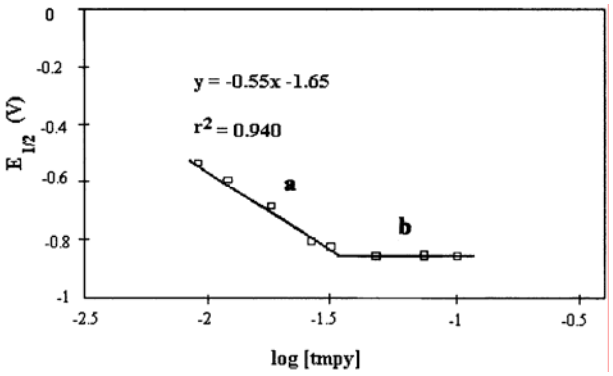

Figure 6. Plot of $E_{1/2}$ for reduction of (a) $OEPFe^{III}Cl$ to $OEPFe^{II}$(tmpy) and (b) $[OEPFe^{III}$(tmpy)Cl to $OEPFe^{II}$(tmpy) *vs.* log[tmpy] in dichloromethane.

mole ratio (Fig. 5f) shifts the reduction wave (c_2) from -0.65 V to -0.88 V. The voltammogram of neat collidine dose not have any reduction wave in that region. Contrary to pyridine, collidine caused cathodic shift in potential of Fe^{III}/Fe^{II} as illustrated in Figure 5.

The plot of changes in $E_{1/2}$ for $a_2 \Leftrightarrow c_2$ couple *vs.* log [collidine] is shown in Figure 6. This plot demonstrates two clear different regions: a and b. In low concentration of collidine, there is a slope of -0.55 mV (part a), corresponding to exchange of one collidine ligand during the reduction process. In part b, which belongs to the high concentration of collidine, the number of exchanged ligands during the reduction process, is zero. Scheme 6 summarizes these observations. Therefore, collidine's effect is different from that of pyridine due to steric hindrance of collidine. Five-coordinate iron(II)-porphinato complexes with aromatic nitrogenous axial ligands, such as pyridine or 1-methylimidazole, bind the second axial ligand 10 to 30 times more avidly than the first, to give thermodynamically and kinetically (d^6, S=0) stable 6-coordinated species process that is avoided by bulky ligands such as collidine and 2-methylimidazole, for which five-coordinate species predominate at room temperature (S=2) even with mild excess of ligand [19,20], (see Scheme 4, 6).

Conclusion

Reduction of $OEPFe^{III}Cl$ in the presence of pyridine, collidine and imidazole in dichloromethane solution was investigated. Addition of pyridine resulted in an anodic shift of potential of Fe^{III}/Fe^{II} whereas for collidine and imidazole a cathodic shift was observed. This suggests that in the presence of pyridine, iron prefers to stay at Fe^{II} level. This odd behavior of pyridine can not be explained solely by the high donor number of pyridine [21,22]. Imidazole and collidine with higher donor numbers, produced different results. π acceptance behavior in pyridine may stabilize $OEPFe^{II}(py)_2$ *vs.* $OEPFe^{III}(py)_2Cl$ and shift potential of Fe^{III}/Fe^{II} toward the anode. It has been found that coupled oxidation, which is a model reaction for heme cleavage, requires pyridine as solvent. Possibly, pyridine is able to preserve the iron in porphyrin at Fe^{II} level, in the presence of O_2/(ascorbic acid). We conclude that Fe^{II} porphyrin is the initial reactor in heme breakdown. In biological systems, protein structure performs this role and Fe^{II} porphyrins are stable in the presence of O_2. Our study on the active reactant in O_2/(reducing agent) system in the heme cleavage process is under progress.

Experimental Section

Chemicals

All reagents and solvents used in this study were prepared from Aldrich Chem. Co. All solvents were spectral graded and dried with phosphorous pentoxide under N_2. TBAP was recrystallized twice from acetaldehyde and n-hexane and crystals of TBAP were saved under vacuums at 40°C under P_2O_5 for two days prior to use.

Electrochemical Measurements

Cyclic voltammogram and pulse polarograph were recorded on a VA-Processor Potentiostat Model 693, VA-Stand Model 694 in a three electrode cell. The working electrode was a platinum disk with a diameter of 2 mm. Before each experiment, the electrode was polished with fine carborundum paper and 0.5 mm alumina slurry in sequence. The electrode was then sonicated in order to remove the trace of alumina from the surface, washed with water and dried. A nonaqueous Ag/AgCl (0.1 M TBACl in CH_2Cl_2) served as the reference electrode. The auxiliary electrode was a platinum electrode. Tetra(n-butyl)ammonium perchlorate (0.1 M) served as the supporting electrolyte. An initial background scan was run to check the purity of the reagents and to establish the solvent's anodic potential range. The cyclic voltammetric scans were started at 0.50 V and increased to -1.00 V. The potential was then reversed. In order to minimize the effect of changing the scan rate on quasi-reversible systems, the scan used in all experiments was 100 mV/s.

Acknowledgements

We thank the Research Council of Shahid Beheshti University for partial financial support.

References

1. Bissel, D. M. In: Ostrow, J. D. (ed.), *Liver: Normal*

function and disease, Vol. 4, Bile Pigments and Juandice, Marcel Decker, Inc., New York, p. 133, (1986).
2. Heirweegh, P. K. and Brown, S. B. In: *Bilirubin, Vol. II, Metabolism.* CRC Press, Florida, p. 1, (1982).
3. Lemberg, R. *Rev. Pure Appl. Chem.*, **6**, 1, (1956).
4. Levin, E. Y. *Biochemistry*, **5**, 2845, (1966).
5. Bonnett, R. and dimsdale, M. J. *J. Chem. Soc. Perkin I*, **79**, 1393, (1972).
6. Saito, S. and Itano, H. A. *Proc. Natl. Acad. Sci., USA*, **79**, 1393, (1982).
7. Lagarias, J. C. *Biochem. Biophys. Acta*, **717**, 12, (1982).
8. Sano, S., Sano, T., Morishima, I., Shiro, Y. and Maeda, Y. *Prec. Natl. Acad. Sci., USA*, 531, (1986).
9. Balch, A. L., Latos-Grazynski, L., Nool, B. C., Olmstead, M. M. and Safari, N. *J. Am. Chem. Soc.*, **115**, 9056, (1993).
10. Balch, A. L., Latos-Grazynski, L., Nool, B. C., Olmstead, M. M., Szterenberg, L. and Safari, N. *Ibid.*, **115**, 1422, (1993).
11. Balch, A. L., Koerner, R., Latos-Grazynski, L., Lewis, J. E., Clair, T. N. S. and Zovinka, E. P. *Inorg. Chem.*, **36**, 3892, (1997).
12. Falk, J. E. In: *Porphyrin and metallporphyrins*, Elsvier, Amsterdam, p. 1, (1964).
13. Clark, W. H. In: *Oxidation and reduction potentials of organic systems*, Baltimore, Md., Williams and Wilkions, p. 1, (1960).
14. Kadish, K. M., Tabard, A., Lee, W., Liu, Y. H., Ratti, C. and Guilard, R. *Inorg. Chem.*, **30**, 1542, (1991).
15. Lever, A. B. P., Gray, H. B. and Kadish, K. M. In: *Iron porphyrin. Part I, II, pp. 173-300*, Addison-Wesley Publishing Company, (1983).
16. Kadish, K. M., Bottomley, L. A. and Beroiz, D. *Inorg. Chem.*, **17**, 1124, (1978).
17. Ann walker, F., Man-Wai Lo and Mully Tutran Ree, *J. Am. Chem. Soc.*, **98**, 5552, (1976).
18. Kadish, K. M. and Bottomley, L. A. *Inorg. Chem.*, **20**, 1348, (1981).
19. Roudee, M. and Brault, D. *Biochemistry*, **14**, 4100-4106, (1975).
20. Bertin, I., Gray, B. H., Lippard, S. J. and Valentine, J. S. In: *Bioinorganic chemistry, p. 200-204*, Valley, M., University Science Book, (1994).
21. Constant, L. A., Davis, D. G. *Anal. Chem.*, **47**, 2253, (1975).
22. Kadish, K. M., Morrison, M. M., Constant, L. A., Dickens, L. and Davis, D. G. *J. Am. Chem. Soc.*, **98**, 8387, (1976).